

# Is Line-of-Sight on Sky Field of View Sufficient to Predict LEO-NTN Communication Availability? Insights from Initial Study Using 360-Degree Camera with Starlink

Naoya Kaneko<sup>\*†</sup>, Rei Nakagawa<sup>†</sup>, Nariyoshi Yamai<sup>†</sup>

<sup>\*</sup> Toyota Motor Corporation, Aichi, Japan      <sup>†</sup> Tokyo University of Agriculture and Technology

**Abstract**—Non-Terrestrial Network (NTN) communications, using Low-Earth Orbit (LEO) satellites, are promising for moving vehicles due to their high-speed, high-capacity communication and wide-area coverage. Meanwhile, in a mobile environment, the rapid relative motion of both satellites and vehicles causes the Line-of-Sight (LOS) to change dynamically, often leading to unexpected communication disruption. To maximize communication opportunities for applications that require stable connectivity, this study proposes an integrated framework that combines vehicle-acquired position, image of sky field of view, satellite orbit, and serving satellite estimation to predict communication availability based on LOS. As an initial study, we verified the relationship between predicting satellite LOS states (active/fading/appearing/hidden) and communication availability through a field test. The experiment involved matching the sky area captured by a 360-degree camera in a stationary environment with Starlink communication. The results indicate that satellite visibility alone cannot fully account for the availability, and by integrating the serving satellite estimation technique, our method can estimate availability with an accuracy of 58.6%.

**Index Terms**—LEO, NTN, Satellites, Communication Availability Prediction

## I. BACKGROUND AND OBJECTIVES

With the widespread use of connected cars, automobiles equipped with communication functions, the emergence of various communication-dependent connected services is imminent [1], [2]. Beyond existing connected services, such as operator assistance and remote air conditioning control, advanced services, such as remote assistance for autonomous vehicles, teleoperation of robotaxis, and telepresence from cars, are anticipated in the future.

Advanced connected services require stable communication while in motion. Current connected cars primarily use 4G/5G cellular mobile services. While the further pervasion of 5G and the market introduction of 6G [3] are promising, coverage holes and weak signal areas are inevitable. To overcome this challenge, communities have been making efforts to use multipath/multi-connectivity communication technologies across multiple cellular networks or to combine heterogeneous wireless communication technologies [4]–[6].

One possible communication path is Non-Terrestrial Networks (NTN), formed by constellations of Low Earth Orbit (LEO) satellites. NTN can provide supplemental communica-

tion services to areas lacking sufficient numbers of cellular base stations or the capacity to cover user terminals (UEs). LEO-NTN offers low-latency communication due to the closer proximity between the ground terminal and satellites, and enables broadband communication by distributing the number of accommodated devices per satellite across large-scale constellations. Currently, Starlink and OneWeb are deployed as commercial services.

While LEO-NTN is promising for connected cars, the mobility of both satellites and vehicles would disrupt stable connectivity due to Line-of-Sight (LOS) loss. Trees, buildings, terrain, and other vehicles, such as trucks, would obstruct LOS between cars and satellites. Our hypothesis in this study is that by predicting LOS loss and recovery, connected cars can fully leverage the potential of LEO-NTN, switching proactively between NTN and the cellular network.

Based on our earlier study [7], we propose a method for predicting LEO-NTN communication availability in response to dynamic changes in LOS. The ground terminal acquires the sky field of view (FOV) image and integrates it with satellite orbit information to determine communication availability. By predicting future LOS for each satellite and the possible accommodating satellite, our method predicts future communication outages and recoveries. Our implementation uses a 360-degree camera, estimates satellite positions from Two Line Element (TLE) data, and classifies each satellite's LOS into several states. The method also introduces the serving-satellite estimation technique proposed in the literature [8].

We evaluated our method in a static field environment. As a result, the system can predict the number of LOS-available satellites within the Starlink antenna's 100-degree FOV with a match rate of 97.45%. For the communication availability prediction, employing only the LOS state estimation achieves 79.7% accuracy but 0.00% specificity, indicating it cannot predict communication outage. In contrast, the serving-satellite estimation technique, when integrated with LOS state estimation, improves the specificity to 44.3%. The low specificity of the former method is due to the finding that, even with more than four satellites in the sky FOV, communication can still experience outages. We assume that Starlink's handover mechanism does not account for the LOS state and may assign

the ground terminal to a satellite that is non-LOS-available.

Key Takeaways and our contributions are as follows:

- Formulating a framework for predicting LEO-NTN communication availability: presenting the overall picture that integrates sky FOV, position information, and satellite orbit estimation.
- Finding that the Starlink handover might not consider LOS between the next satellite and the ground terminal.
- Limitations of the LOS states-only prediction: achieves an accuracy of 79.7%; however, it fails to predict communication outage, as there are consistently more than several satellites in the sky region.
- Effectiveness of the serving-satellite estimation: the method can achieve a prediction accuracy of 58.6%, a precision of 80.7%, and a recall of 62.4%, although the apparent accuracy value is lower than the LOS states only method due to evaluation environment characteristics.

This paper is structured as follows. Section 2 describes related research. Section 3 presents an overview of the proposed method. Section 4 evaluates the system that implements the proposed method and discusses the evaluation results. Finally, we conclude this paper and elaborate on future challenges.

## II. RELATED WORK

Numerous studies have examined the communication characteristics of the Starlink service, which our study also targets.

The literature [9] measures connectivity, RTT, throughput, and network routes from Starlink antennas at four locations to AWS regions around the globe, reports comparisons with terrestrial networks, and discusses the impact of terrain-induced LOS loss. Additionally, the work discusses communication quality in vehicle environments, based on RTT and throughput measurements. Our study similarly assumes terrain as an obstacle that vehicles may encounter. We propose predicting changes in communication availability caused by obstructions, such as buildings and large adjacent vehicles.

The literature [8] models the selection of handover destination satellites in Starlink with the help of machine-learning techniques, from features such as satellite elevation angle, direction of arrival, launch year, and presence of sunlight, and evaluates the estimation accuracy of serving-satellites using the top-k accuracy metric. Also, the literature reports a global handover schedule for every 15 seconds. While the study uses Starlink's Obstruction Map, our method uses the camera view. The Obstruction Map assumes operation in fixed environments and requires about 1 hour to calculate LOS around the site. In contrast, our method acquires visibility information immediately and is effective for mobility use cases. Our method draws on the literature for estimating connected satellites to improve the accuracy of communication availability prediction.

The literature [10] proposes a method to improve GPS positioning accuracy by capturing the sky FOV using an infrared camera and excluding multipath-affected signals from non-LOS-available satellites. Our study focuses on communication satellites and predicts communication availability by combining future satellite positions and the sky FOV. On the

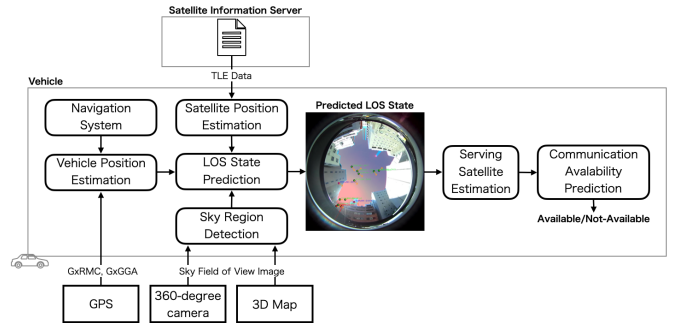


Fig. 1: Overview of the proposed method

other hand, the technique using infrared cameras improves the accuracy of sky-region detection at night and is applicable to our method as well.

The literature [11] proposes a sky-region detection method from a single VGA (640x480) image, achieving high detection accuracy (95%) and short processing time (150ms). Our method applies the technique to images from a 360-degree camera of the sky FOV.

## III. PROPOSED METHOD

This section describes the LEO-NTN communication availability prediction method, integrating vehicle position, the sky FOV from mobility, and satellite orbit estimation. Figure 1 shows the overview of the proposed method.

The key idea of our method is that, for mobile objects like vehicles where LOS conditions change rapidly, the availability of LEO-NTN can be determined and predicted by inferring the LOS state from the sky-region within the sky field and satellite positions. The method consists of the following elements.

- 1) Vehicle Position Estimation: acquire and estimate current and future vehicle position from a GPS device or a navigation system
- 2) Sky-Region Detection: acquire the sky FOV image for the current and future position from a 360-degree camera and a 3D map, and detect the sky-region where no obstruction is present.
- 3) Satellite Position Estimation: acquire TLE data from the satellite information server and estimate current and future position for each satellite.
- 4) LOS State Prediction: integrate vehicle position, satellite position, and sky-region to estimate and predict LOS state for each satellite.
- 5) Serving-Satellite Estimation: estimate candidates for serving-satellite that the Starlink network has assigned the ground terminal to.
- 6) Communication Availability Prediction: predict network availability from the LOS states for the candidate serving-satellites.

Our method assumes that vehicles communicating through the Starlink network are also equipped with a GPS positioning and navigation system, enabling acquisition of latitude, longitude, altitude, direction, speed, and time. The vehicle position

**TABLE I:** LOS State based on satellite position and inclusion in the sky-region

	Current position is included	Current position is not included
Future position is included	active	appearing
Future position is not included	fading	hidden

estimation provides position and motion information for the current and future time. For vehicles, route information from the navigation system is available to predict future positions for long-term prediction.

To obtain the satellite-visible sky-region, the vehicle uses a camera to capture the sky FOV or relies on 3D maps to estimate future sky visibility. Sky-region detection then identifies unobstructed areas via image processing. The camera can be a standard camera, such as a dashboard camera or a 360-degree camera for full-surround capture. Additionally, transportation digital twins can also provide 3D map data.

Our method defines a satellite information server as a server that provides TLE or related satellite orbit data. For example, CelesTrak<sup>1</sup> and SPACE-TRACK.ORG<sup>2</sup> publish TLE data, including LEO satellites for Starlink, OneWeb, and Kuiper. SpaceX also publishes ephemeris data for its satellites, including minute-by-minute positions and velocities for the next three days.

By integrating vehicle position, the sky-region, and satellite position, our method estimates the current and future LOS states for each satellite. First, the LOS state prediction converts satellite positions to relative positions within the image of the sky FOV. Secondly, satellite positions are checked to determine whether they are in the sky-region and classified into four states. Table I shows the four states: *active*, *appearing*, *fading*, and *hidden*. In addition to the LOS state, our method similarly determines whether each satellite is within the beam width (100 degrees) or antenna FOV; *active beam*, *appearing beam*, *fading beam*, and *hidden beam*.

The serving-satellite estimation narrows down the possible connecting satellite from the LOS state predicted satellites. By employing the rule-based estimation technique derived from the literature [8], our method estimates the current and next serving satellite candidate lists every 15 seconds during Starlink's global handover period. The estimated serving-satellites list consists of up to five satellites, each assigned a score representing the likelihood of being a serving-satellite on a scale of 0 to 100.

Finally, based on the LOS states and the estimated serving-satellite list, the communication availability prediction determines whether the high-score-likelihood serving-satellites are in an *active beam* or *fading beam* state. Algorithm 1 shows the algorithm for the prediction. If the score is 85 or higher, the corresponding satellite is considered a serving-satellite. If

**Algorithm 1** Prediction of communication availability based on sky-region, TLE Data and serving-satellite estimation

---

**Require:** Set of TLE data  $\mathcal{L}$ , current time  $T$ , prediction target time  $T_{\text{pred}}$ , threshold  $\tau$  (e.g.,  $\tau = 85$ )

**Ensure:** available: Boolean indicating predicted communication availability

```

1:  $T_{\text{HO}} \leftarrow \text{GETNEXTHANDOVERTIME}(T)$ 
2: pos  $\leftarrow \text{GetPosition}(T_{\text{pred}})$ 
3: img  $\leftarrow \text{GETSKYFOV}(T_{\text{pred}})$ 
4: losStates  $\leftarrow \text{ESTIMATELOSSTATE}(\mathcal{L}, T_{\text{pred}}, \text{img}, \text{pos})$ 
5: cands  $\leftarrow \text{ESTIMATESERVINGSATELLITES}(\mathcal{L}, T_{\text{HO}}, \text{pos})$ 
6: sats  $\leftarrow \emptyset$ 
7: for sat  $\in$  cands do
8:   if sat.score  $\geq \tau$ 
9:     and ISACTIVEORFADING(losStates, sat) then
10:    sats  $\leftarrow$  sats  $\cup$  {sat}
11:   end if
12: end for
13: return IsEmpty(sats)

```

---

**TABLE II:** Hardware configuration

Component	Hardware
Communication	Starlink Mini
GPS	GR-8017 (USB, u-blox M8U)
360-degree camera	RICOH THETA S
PC	MacBookPro (M3 Pro)

one or more of these satellites are in a LOS state of *active beam* or *fading beam*, communication is deemed available.

#### IV. IMPLEMENTATION

The section describes the system implementation of our proposed method. At the time of writing, Starlink prohibits its use in motion due to local regulations in Japan<sup>3</sup>. Thus, our system focuses on a static environment.

Our system uses a USB-GPS device for vehicle position, a 360-degree camera for the sky FOV image, and CelesTrak's website as the satellite information server. The hardware configuration used for implementing the proposed method is described in Table II. Our system assumes that the 360-degree camera is installed facing the zenith from the GPS-indicated position, capturing the sky FOV from the current position.

For sky-region detection, the system acquires images from the THETA S with OpenCV. As shown in Figure 2, the image from the HDMI output port of THETA S is a double-fisheye, equidistant projection. Our implementation converts the image into an equirectangular projection and then detects the sky region. For the detection, our system uses the open-source implementation<sup>4</sup> of the technique in the literature [11].

TLE data is acquired from CelesTrak's NORAD GP Element Sets Current Data<sup>5</sup>. Since TLE data is updated approx-

<sup>1</sup><https://celesttrak.org/>

<sup>2</sup><https://www.space-track.org/>

<sup>3</sup><https://starlink.com/support/article/50e933eb-54f5-1a77-cc85-c6c8325564cf> (accessed 2025/10/19)

<sup>4</sup><https://github.com/cftang0827/sky-detector>

<sup>5</sup><https://celesttrak.org/NORAD/elements/>



Fig. 2: Double fisheye image from RICOH THETA S

imately once per day, our system assumes that the data is downloaded and cached in advance using satellite or cellular mobile communication before processing. Our system employs Python’s Skyfield library<sup>6</sup> for processing the TLE data. TLE data for each satellite record is up to 160 bytes, totaling about 1 MB for all satellites. SpaceX publishes further accurate ephemeris data<sup>7</sup>; however, the size for each satellite is about 2MB, which adds up to 16GB in total. Thus, for a resource-limited vehicle environment, we choose to use TLE data.

## V. EVALUATION

This section evaluates the implemented system based on the following perspectives:

- 1) Accuracy of LOS states prediction: How accurately can our system predict the future LOS state for the satellites?
- 2) Relation of LOS state and communication availability: Is LOS state sufficient to predict communication outage and recovery?
- 3) Effect of serving-satellites estimation technique: To what extent can rule-based estimation of serving-satellites help improve communication availability prediction?

In this paper, we predict communication availability based on LOS state and estimates of serving-satellites. The error between the predicted future LOS state of satellites at a specific time point and the actual state generates prediction errors. By verifying the prediction accuracy of LOS states, we clarify the error contained in the system. By examining the relationship and transition between satellite LOS states and network reachability tests, we clarify the impact of LOS states on communication availability. Finally, by analyzing the use of the serving-satellite estimation technique in combination with LOS state prediction, we determine whether the estimation improves prediction.

### A. Evaluation Environment

The evaluation setup is shown in Figure 3. We installed the 360-degree camera in a fixed direction so that the top of the double fisheye image points east.

For the experiment, we select a location with obstructions; the sky FOV from the location is shown in Figure 4. The location is on the balcony of a mid-level floor of a building, with the eastern sky obstructed by buildings. Approximately

<sup>6</sup><https://rhodesmill.org/skyfield/>

<sup>7</sup><https://api.starlink.com/public-files/ephemerides/MANIFEST.txt>

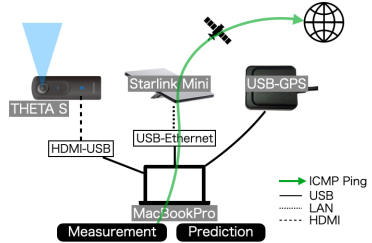


Fig. 3: Evaluation environment configuration in static environment



Fig. 4: Sky FOV in evaluation environment

53% is a sky-region. We conduct the measurement between 6:00 and 7:00 PM under clear weather conditions.

We run the system to predict the LOS state at 2-second intervals for the current and 10 seconds after, and, in parallel, we use ICMP ping to measure communication availability and RTT to the Internet via Starlink. For each cycle, the system records the image obtained from the 360-degree camera, the sky region detection result image, the position and state of each satellite, the estimated serving-satellites list, and an image plotting satellites color-coded by LOS state and their future positions, on top of the sky region on the camera image.

### B. Accuracy of satellite LOS state prediction

Figures 5 and 6 compare the predicted and actual transitions of LOS-available satellites classified as *active* or *fading*, as well as their antenna FOV counterparts (*active beam*, *fading beam*). Figure 5 shows satellites whose future positions overlap with the detected sky-region, while Figure 6 further restricts the comparison inside the antenna FOV. Throughout the experiment period, there are no events in which all satellites disappeared entirely from the sky-region or antenna FOV. In general, more than 30 satellites are visible in the sky, and more than four are continuously present within antenna FOV.

Figure 7 shows an example of the current and predicted LOS states during the experiment. In the plot, the red background indicates the sky-region detected from the 360-degree camera image. Each circle represents a satellite, with its color denoting the LOS state classification: green for *active*, blue for *appearing*, red for *fading*, and black for *hidden*. The circle’s border color further shows whether the satellite lies within the antenna FOV, and orange arrows depict future satellite

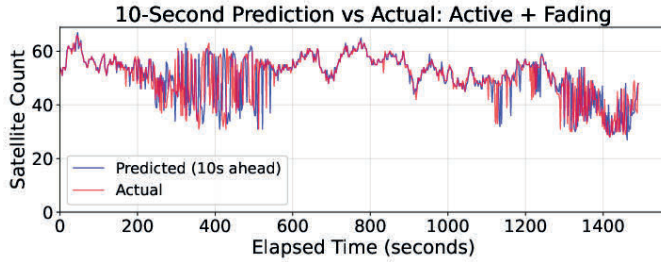


Fig. 5: Actual and predicted numbers of satellites with LOS

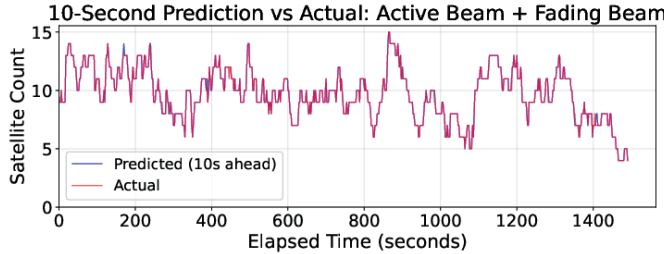


Fig. 6: Actual and predicted numbers of satellites with LOS and within antenna FOV

positions. The plot also provides identification numbers and azimuth/elevation labels for reference.

We evaluate LOS prediction accuracy using the *match rate*, defined as the fraction of time the predicted and actual numbers of LOS-available satellites match. The match rates are 42.86% for all LOS-available satellites and 97.45% within antenna FOV. The root mean square errors are 6.99 and 3.56, and the mean absolute errors are 0.15 and 0.02, indicating high accuracy when limited to the antenna FOV.

The primary error sources are inaccuracies in sky-region detection and image distortion from the 360-degree fisheye cameras. As shown in Figure 7, clouds and color gradients lead to misdetection near sky-region boundaries. Using a machine-learning-based sky segmentation method [12] could improve detection accuracy. Furthermore, our satellite coordination transformation assumes an equidistant projection, whereas fisheye lenses can introduce nonlinear distortion. Applying a correction technique [13] can reduce these geometric errors and improve LOS state prediction.

### C. Relation of LOS state and communication availability

Are LOS states sufficient to predict communication outage and recovery in LEO-NTN? That is the key question in this paper. To examine the question, we compare the occurrence of ping-loss events with the transitions of LOS-active satellites. A simple assumption is that if there are no LOS-available satellites in the sky, communication is also unavailable, and that the converse is also true.

Figure 8 and 9 show the transition of the number of LOS-available satellites within the sky region and the antenna FOV as a line chart, the ping loss event in a red bar, and the global handover time of Starlink in the purple vertical line.

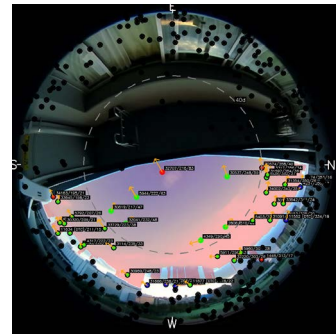


Fig. 7: Example plot of current and predicted LOS states

TABLE III: Metrics for prediction effectiveness

	A. LOS state only	B. LOS state within beam	C. LOS state within beam & serving-satellite estimation	D. Random
Accuracy[%]	79.7	79.7	58.6	49.4
Precision[%]	79.7	79.7	80.7	53.3
Recall[%]	100.0	100.0	62.4	49.6
F-measure	0.88	0.88	0.70	0.51
Specificity[%]	0.00	0.00	44.3	49.1
Balanced Accuracy[%]	50.0	50.0	53.4	49.4
ROC-AUC	0.50	0.50	0.53	0.49

In both figures, ping loss occurs or persists even when one or more LOS-available satellites are available, which are considered capable of providing connectivity. Therefore, while LOS is effective for detecting worst-case scenarios where no satellites are present, it is not a sufficient condition for predicting communication availability. The result suggests that Starlink can allocate the ground terminal to the satellite in a *hidden* or *hidden beam* state during every 15-second periodic handover event. During the experiment period, we observed 40 transitions from ping OK to ping NG. Still, upon closer inspection, we confirmed that no satellites became hidden or fell outside the antenna FOV.

The other elements, such as network congestion within the Starlink network, signal interference, multipath fading, and errors in sky-region detection, might have contributed to the communication outage. Further inspection and analysis of the possible reason are required.

### D. Effect of serving-satellites estimation technique

Table III summarizes the evaluation metrics for four prediction methods: LOS state only prediction (A), LOS within antenna FOV (B), LOS combined with serving-satellite estimation (C), and random prediction (D). The purpose of the comparison is to validate the predictive capability of our proposed method (C) against others. The metrics comparison includes accuracy, precision, recall, F-measure, specificity, balanced accuracy, and ROC-AUC.

Methods A and B achieved high accuracies of 79.7%; however, both exhibit 100.0% recall and 0.00% specificity, indicating that both predicted communication as always available.

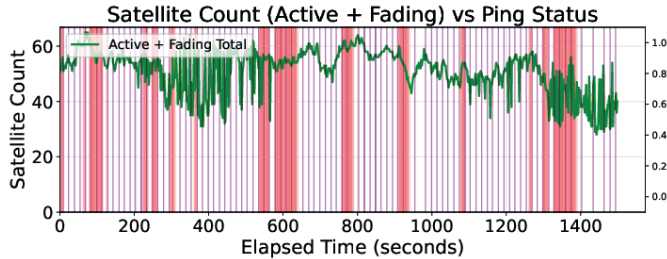


Fig. 8: Transition of the number of LOS-available satellites with LOS and ping loss occurrence

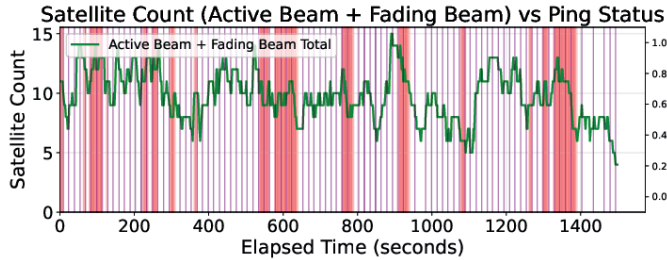


Fig. 9: Transition of the number of LOS-available satellites within antenna FOV and ping loss occurrence

The high values reflect the dataset imbalance in the experiment environment, where communication is more available than disrupted, and do not imply predictive capability.

Method D, a pure random predictor, achieved accuracy of 49.4%, precision of 53.3%, recall of 49.6%, specificity of 49.1%, and ROC-AUC of 0.49 for a 10-times average. The result establishes the lower bound of prediction performance.

Our method, C, shows accuracy of 58.6%, precision of 80.7%, recall of 62.4%, and specificity of 44.3%, resulting in balanced accuracy of 53.36% and ROC-AUC of 0.53. The result indicates a slight but statistically significant improvement over random prediction, suggesting that integrating serving-satellite estimation enhances predictive capability. Although the performance remains limited, the result demonstrates that rule-based serving-satellite estimation captures part of the underlying pattern compared to the LOS states-only method.

Further evaluation is necessary due to the limited experiment in this paper. The different sky FOV in various locations may show different results. For example, different obstructions might affect the estimation accuracy.

## VI. CONCLUSION AND FUTURE WORK

In this paper, we brought a hypothesis that LOS states of each satellite within the vehicle's sky FOV can predict LEO-NTN communication availability. In the course of examining this hypothesis, we proposed a framework for prediction that integrates vehicle position, the sky FOV, and satellite position. We focus on satellites of the Starlink network, plotting their current and future positions in the sky from a 360-degree camera image and classifying their LOS states. Our field evaluation confirmed that LOS states alone cannot predict communication availability, and our hypothesis was

false. However, by employing the serving satellite estimation technique, our system can achieve better prediction, achieving accuracy for 58.6%, precision for 80.7%, recall for 62.4%, and specificity for 44.3%.

Future work includes improving prediction accuracy by incorporating a machine-learning-based serving satellite estimation technique into our framework. Our current implementation only uses rule-based estimation, and further adaptation of the technique in the literature [8] is promising. Additionally, as our prediction evaluation is limited to static environment results, further experiments in a moving environment and improvement of the method are necessary. Last but not least, we aim to explore practical integration with a multipath scheduler, enabling our LOS-based availability prediction to inform proactive path selection for multi-connectivity.

## REFERENCES

- [1] Automotive Edge Computing Consortium, "General Principles and Vision (Paper) Version 4.0.4." [Online]. Available: <https://aec.org/resources/publications/>
- [2] 5G Automotive Association, "Toward fully connected vehicles: Edge computing for advanced automotive communications." [Online]. Available: <https://5gaa.org/5gaa-in-motion/news/#white-papers>
- [3] I. Tomkos, D. Klonidis, E. Pikasis, and S. Theodoridis, "Toward the 6g network era: Opportunities and challenges," *IT Professional*, vol. 22, no. 1, pp. 34–38, 2020.
- [4] B. Hu, X. Zhang, Q. Zhang, N. Varyani, Z. M. Mao, F. Qian, and Z.-L. Zhang, "Leo satellite vs. cellular networks: Exploring the potential for synergistic integration," in *Companion of the 19th International Conference on Emerging Networking EXperiments and Technologies*, ser. CoNEXT 2023. New York, NY, USA: Association for Computing Machinery, 2023, p. 45–51.
- [5] A. Ramírez-Arroyo, T. B. Sørensen, and P. Mogensen, "Terrestrial 5g and starlink ntn multi-connectivity toward 6g communications integration era: An empirical assessment," *IEEE Open Journal of the Communications Society*, vol. 6, pp. 5269–5283, 2025.
- [6] Y. Komatsu, D. Cavendish, D. Nobayashi, and T. Ikenaga, "Multipath TCP video streaming hand-offs on LEO satellite/5G cellular networks," *PacRim*, pp. 1–6, Aug. 2024.
- [7] N. Kaneko, R. Nakagawa, and Y. Nariyoshi, "Leo ntn communication availability prediction method by integrating sky field of view from mobility and satellite orbit prediction: Initial study using a 360-degree camera," *Information Processing Society of Japan, Tech. Rep.* 2025-IOT-71, Sep 2025.
- [8] H. B. Tanveer, M. Puchol, R. Singh, A. Bianchi, and R. Nithyanand, "Making sense of constellations: Methodologies for understanding starlink's scheduling algorithms," in *Companion of the 19th International Conference on Emerging Networking EXperiments and Technologies*, ser. CoNEXT 2023. New York, NY, USA: Association for Computing Machinery, 2023, p. 37–43.
- [9] S. Ma, Y. C. Chou, H. Zhao, L. Chen, X. Ma, and J. Liu, "Network characteristics of leo satellite constellations: A starlink-based measurement from end users," in *IEEE INFOCOM 2023 - IEEE Conference on Computer Communications*, 2023, pp. 1–10.
- [10] J.-i. Meguro, T. Murata, J.-i. Takiguchi, Y. Amano, and T. Hashizume, "Gps accuracy improvement by satellite selection using omnidirectional infrared camera," in *2008 IEEE/RSJ International Conference on Intelligent Robots and Systems*, 2008, pp. 1804–1810.
- [11] Y. Shen and Q. Wang, "Sky region detection in a single image for autonomous ground robot navigation," *International Journal of Advanced Robotic Systems*, vol. 10, no. 10, p. 362, 2013.
- [12] R. P. Mihail, S. Workman, Z. Bessinger, and N. Jacobs, "Sky segmentation in the wild: An empirical study," in *IEEE Winter Conference on Applications of Computer Vision (WACV)*, 2016, pp. 1–6.
- [13] D. Scaramuzza, A. Martinelli, and R. Siegwart, "A toolbox for easily calibrating omnidirectional cameras," in *2006 IEEE/RSJ International Conference on Intelligent Robots and Systems*, 2006, pp. 5695–5701.